

Characterization of the healing process in non-stabilized and stabilized femur fractures in mice

T. Histing¹ · K. Heerschop¹ · M. Klein¹ · C. Scheuer² · D. Stenger¹ · J. H. Holstein¹ · T. Pohlemann¹ · M. D. Menger²

Received: 30 June 2015 / Published online: 24 November 2015
© Springer-Verlag Berlin Heidelberg 2015

Abstract

Background Although a variety of suitable fracture models for mice exist, in many studies bone healing was still analyzed without fracture stabilization. Because there is little information whether the healing of non-stabilized fractures differs from that of stabilized fractures, we herein studied the healing process of non-stabilized compared to stabilized femur fractures.

Materials and methods Twenty-one CD-1 mice were stabilized after midshaft fracture of the femur with an intramedullary screw allowing micromovements and endochondral healing. In another 22 mice the femur fractures were left unstabilized. Bone healing was studied by radiological, biomechanical, histomorphometric and protein expression analyses.

Results Non-stabilized femur fractures revealed a significantly lower biomechanical stiffness compared to stabilized fractures. During the early phase of fracture healing non-stabilized fractures demonstrated a significantly lower amount of osseous tissue and a higher amount of cartilage tissue. During the late phase of fracture healing both non-stabilized and stabilized fractures showed almost 100 % osseous callus tissue. However, in stabilized fractures remodeling was almost completed with lamellar bone while non-stabilized fractures still showed large callus with great amounts of woven bone, indicating a delay in bone remodeling. Of interest, western blot analyses of callus

tissue demonstrated in non-stabilized fractures a significantly reduced expression of vascular endothelial growth factor and a slightly lowered expression of bone morphogenetic protein-2 and collagen-10.

Conclusion Non-stabilized femur fractures in mice show a marked delay in bone healing compared to stabilized fractures. Therefore, non-stabilized fracture models may not be used to analyze the mechanisms of normal bone healing.

Keywords Non-stabilization · Stabilization · Fracture · Mice · Bone remodeling

Introduction

Despite the progress in understanding the mechanisms of fracture healing, delayed bone healing still occurs in approximately 10 % of long bone fractures and, thus, represents a significant public health problem [1]. The causes of delayed healing and non-union are multifactorial and not completely understood yet. This forces further in vivo research with the use of adequate animal models.

During the last three decades a considerable number of animal models have been introduced to study the mechanisms of bone healing. In the past, large animal models were preferentially used [2–4]. This was mainly because the process of bone healing in sheep, dogs and pigs was thought to more closely mimic that in humans compared to rodents. In addition, both the implants for stabilization and the associated surgical procedures could be easily transferred through the knowledge available from the daily clinical practice.

During the last decade, however, mouse models have gained increasing interest in orthopedic research. This is

✉ T. Histing
tina.histing@uks.eu

¹ Department of Trauma, Hand and Reconstructive Surgery, Saarland University, 66421 Homburg/Saar, Germany

² Institute for Clinical and Experimental Surgery, Saarland University, 66421 Homburg/Saar, Germany

due to the large number of genetically manipulated animals and the broad spectrum of antibodies available, which allow distinct analyses of molecular mechanisms of fracture healing [5]. On the other hand, the use of mice for fracture healing research is highly challenging, because the small size of the bones requires sophisticated osteosynthesis techniques to mimic the clinical situation in humans. Accordingly, in some early studies on fracture healing in mice, the fractured bones were left unstabilized [6, 7]. Meanwhile, however, a variety of suitable osteosynthesis techniques in mice have been introduced [8–11], allowing the study of both endochondral and intramembranous bone healing. Despite these advances and the knowledge that biomechanical factors substantially influence the process of bone healing [12], non-stabilized fractures in mice are still used to study the mechanisms of bone healing [13, 14].

In fact, little is known whether the healing process in non-stabilized fractures differs from that of stabilized fractures. Le et al. [15] analyzed the molecular gene expression in stabilized and non-stabilized tibia fractures in mice and could demonstrate a more pronounced indian hedgehog expression in non-stabilized fractures, which was associated with a delay in chondrocyte differentiation. In addition, Lu et al. [16] found that the instability of non-stabilized fractures promotes angiogenesis during early healing process. However, it is not known whether non-stabilized fractures show an altered osseous healing and remodeling compared to stabilized fractures in mice. Therefore, we herein studied callus formation, biomechanical callus stability and callus remodeling during the healing process of non-stabilized versus stabilized femur fractures in mice.

Materials and methods

Animals

A total of 43 4-month-old female CD-1 mice with a body weight (BW) of 33 ± 0.4 g were used for the study. The animals were kept in standard cages at a 12-h light and dark cycle. They were fed a standard pellet diet (Altromin, Lage, Germany) and had free access to tap water. The study was approved by the governmental animal care committee. All procedures were performed according to the National Institute of Health guidelines for the use of experimental animals (No. 07/2013, revised 2007).

Surgical procedure

Mice were anesthetized by an intraperitoneal injection of xylazine (15 mg/kg BW) and ketamine (75 mg/kg BW). The stabilization of femur fractures was performed with

the MouseScrew ($n = 21$) allowing micromovements at the fracture site and, thus, endochondral healing [11]. Therefore, a 4 mm medial parapatellar incision was performed under sterile conditions at the right knee to dislocate the patella laterally. After drilling a hole (0.5 mm in diameter) into the intercondylar notch, an injection needle with a diameter of 0.4 mm was drilled into the intramedullary canal. Subsequently, a tungsten guide wire (0.2 mm in diameter) was inserted through the needle into the intramedullary canal. After removal of the needle, the femur was fractured by a 3-point bending device and an intramedullary medical grade stainless steel screw (17.2 mm length, 0.5 mm in diameter) was implanted over the guide wire to stabilize the fracture [17]. The screw consisted of a distal cone-shaped head (diameter 0.8 mm) and a proximal thread (M 0.5 mm, length 4 mm) allowing fracture compression (Research Implants Systems (RIS), Davos, Switzerland). After fracture fixation, the wound was closed using 6-0 synthetic sutures. Fracture and implant position were confirmed by radiography (MX-20, Faxitron X-ray Corporation, Wheeling, IL, USA). In the non-stabilized fracture group ($n = 22$), femora were also fractured by a 3-point bending device and were left unstabilized. Fracture configuration was documented by radiography.

For analgesia the mice received tramadol-hydrochloride (Grünenthal, Aachen, Germany) in the drinking water (40 mg/100 ml) from day 1 before surgery until day 3 after surgery. If needed (lack of mobility), analgesia was continued until the animals showed normal behaviour including feeding, cleaning and sleeping habits. To facilitate food intake during the postoperative period, cages were used in which the food racks of the caps extend into the cage to such a degree that the animals could eat and drink in lying position. During the early postoperative period, food pellets and solid drinks (Triple A Trading, Tiel, The Netherlands) were additionally placed directly in the cage.

Experimental protocol

Twenty-one mice were stabilized with the intramedullary screw. Two weeks after fracture, nine of these mice were killed for radiological, biomechanical and histomorphometrical analysis. Four additional mice were killed for protein biochemical analysis. The remaining eight mice were killed after 5 weeks of fracture healing for radiological, biomechanical and histomorphometrical analysis. In 22 additional mice the femur fractures were left unstabilized. Two weeks after fracture, eight of these mice were killed for radiological, biomechanical and histomorphometrical analysis. Four additional mice were killed for protein biochemical analysis. The remaining ten mice were

killed after 5 weeks of fracture healing for radiological, biomechanical and histomorphometrical analysis.

Radiological analysis

At 2 and 5 weeks after fracture, animals were anesthetized and ventro-dorsal X-rays (MX-20, Faxitron) of the fractured femora were performed. Fracture repair was analyzed according to the Goldberg classification with stage 0 indicating radiological non-union, stage 1 indicating possible union and stage 2 indicating radiological union [18].

Biomechanical analysis

For biomechanical analysis, the right femora were resected at 2 and 5 weeks and freed from soft tissue. In the group with stabilized fractures the screws were removed before testing. Callus stiffness was measured with a non-destructive bending test using a 3-point bending device (Mini-Zwick Z 2.5, Zwick GmbH, Ulm, Germany) [17]. Due to the different states of healing (2 vs. 5 weeks), the loads which had to be applied varied markedly between the individual animals. Loading was stopped individually in every case when the actual load–displacement curve deviated more than 1 % from linearity. To guarantee standardized measuring conditions, femora were mounted always with the ventral aspect upwards. A working gauge length of 6 mm was used. Applying a gradually increasing bending force with 1 mm/min, the bending stiffness (N/mm) was calculated from the linear elastic part of the load–displacement diagram. Control that the load was not destructive was performed macroscopically and microscopically (histology).

Histomorphometrical analysis

For histology, bones were fixed in IHC zinc fixative (BD Pharmingen, Heidelberg, Germany) for 24 h, decalcified in 10 % EDTA solution for 2 weeks and then embedded in paraffin. Longitudinal sections of 5 μ m thickness were stained according to the trichrome method (Masson-Goldner). At a magnification of 12.5 \times (Olympus BX60 Microscope, Olympus, Tokyo, Japan; Zeiss Axio Cam and Axio Vision 3.1, Carl Zeiss, Oberkochen, Germany) structural indices were calculated according to the suggestions provided by Gerstenfeld et al. [19] using the ImageJ Analysis System (NIH, Bethesda, MD, USA). These included total callus area (bone, cartilaginous and fibrous callus area)/femoral bone diameter (cortical width plus marrow diameter) at the fracture gap [CAr/BDm (mm)], bone (total osseous tissue) callus area/total callus area [TOTAr/CAr (%)] and cartilaginous callus area/total callus area [CgAr/CAr (%)].

Western blot analysis

The expression of bone morphogenetic protein (BMP)-2, collagen 2 and 10, cysteine-rich protein (CYR) 61, vascular endothelial growth factor (VEGF), receptor activator of nuclear factor κ B ligand (RANKL) and osteoprotegerin (OPG) was analyzed by western blotting. Therefore, the callus tissue was frozen and stored at -80°C until further processing. For whole protein extracts the callus tissue was homogenized in lysis buffer (10 mM Tris pH 7.5, 10 mM NaCl, 0.1 mM EDTA, 0.5 % Triton-X 100, 0.02 % NaN_3 , 0.2 mM PMSF), and protease inhibitor cocktail (1:75 v/v; Sigma-Aldrich, Taufkirchen, Germany), phosphatase inhibitor cocktail (1:100 v/v; Sigma-Aldrich), incubated for 30 min on ice and centrifuged for 30 min at 16,000 \times g. Protein concentrations were determined using the Lowry assay. The whole protein extracts (10 μ g protein per lane) were separated discontinuously on sodium dodecyl sulfate polyacrylamide gels and transferred to polyvinylidene difluoride membranes. After blockade of non-specific binding sites, membranes were incubated with the following antibodies: rabbit anti-mouse BMP-2 (1:100, 3.5 h at room temperature and 1:50 over night at 4°C , Santa Cruz Biotechnology, Heidelberg, Germany), rabbit anti-mouse collagen-2 and -10 (1:300, 3.5 h at room temperature and 1:50 over night at 4°C , Bioss by Biozol, Eching, Germany), goat anti-mouse CYR61 (1:100, 3.5 h at room temperature and 1:50 over night at 4°C , Santa Cruz Biotechnology), rabbit anti-mouse VEGF (1:100, 3.5 h at room temperature and 1:50 over night at 4°C , A20, Santa Cruz Biotechnology), rabbit anti-mouse RANKL (1:500, 3.5 h at room temperature and 1:100 over night at 4°C , Abcam, Cambridge, UK) and rabbit anti-mouse OPG (1:500, 3.5 h at room temperature and 1:100 over night at 4°C Bioss by Biozol). This was followed by corresponding horseradish peroxidase-conjugated secondary antibodies (1.5 h, 1:5000, GE Healthcare, Freiburg, Germany). Protein expression was visualized using luminol-enhanced chemiluminescence (ECL, GE Healthcare). Signals were densitometrically assessed (Quantity one, Geldoc, BioRad, München, Germany) and normalized to β -actin signals (1:5000, mouse–anti-mouse β -actin, Sigma-Aldrich) to correct for unequal loading.

Statistical analysis

All data are given as mean \pm SEM. After proving the assumption for normal distribution (Kolmogorov–Smirnov test) and equal variance (F test), comparison between the two experimental groups was performed using Student's t test. For non-parametrical data Mann–Whitney U test was used. Statistics were performed using the SigmaPlot 13.0 software (Systat Software GmbH, Erkrath, Germany). A p value <0.05 was considered to indicate significant differences.

Results

Radiological analysis

Radiological analyses at 2 and 5 weeks demonstrated a lower Goldberg score of non-stabilized femur fractures compared to fractures after intramedullary screw fixation (Table 1). At 2 weeks the non-stabilized fractures showed an obvious dislocation of the fragments with a large, irregular callus configuration (Fig. 1a). At 5 weeks, massive callus was still detectable at the fracture site and the remodeling process was not completed (Fig. 1b). In contrast, at 2 weeks stabilized fractures were found adequately reduced with regular callus formation (Fig. 1c). At 5 weeks the fracture was healed and the process of remodeling was almost completed (Fig. 1d).

Biomechanical analysis

At 2 weeks after fracture, the bending stiffness of the non-stabilized femur fractures was significantly lower

Table 1 Radiological analysis at 2 and 5 weeks after fracture according to the Goldberg-score of non-stabilized and stabilized femur fractures

	Non-stabilized	Stabilized
2 weeks	0.5 ± 0.2*	1.0 ± 0.0
5 weeks	1.5 ± 0.2*	2.0 ± 0.0

Mean ± SEM

* $p < 0.05$ vs. stabilized femur fractures

compared to that after intramedullary screw fixation (Fig. 2). At 5 weeks, the bending stiffness of non-stabilized fractures was still 50 % lower when compared to that of screw fixed fractures (Fig. 2).

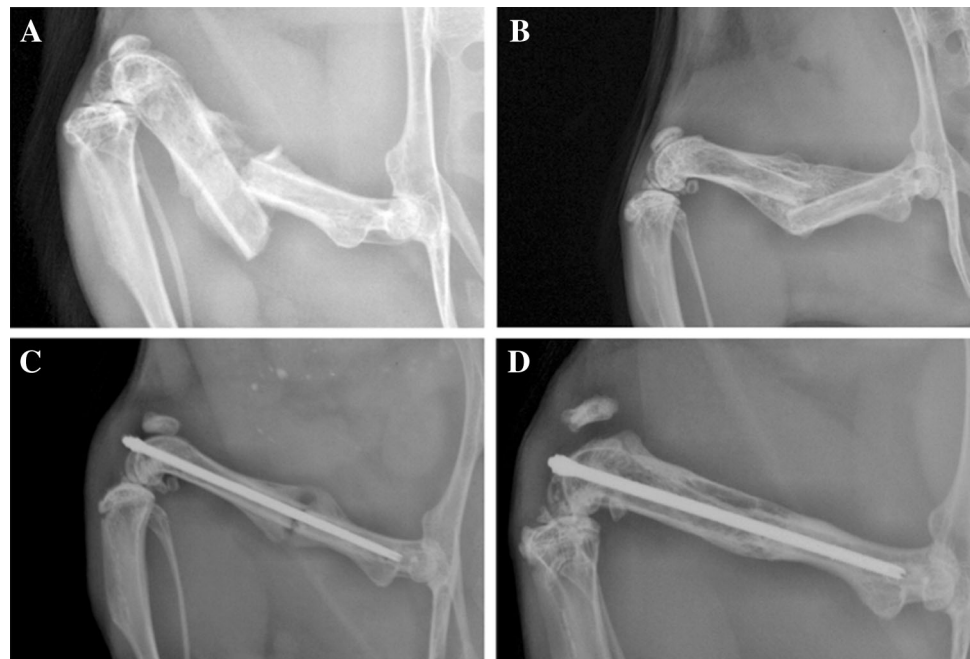
Histological analysis

Analysis of the total callus area in relation to the femoral diameter indicated that the callus size of non-stabilized femur fractures was significantly larger at 2 weeks as well as at 5 weeks after fracture (Figs. 3a, 4a–d). At 2 weeks after fracture the non-stabilized fractures showed a significantly lower amount of newly formed bone (Figs. 3b, 4a, c) as well as a significantly higher amount of cartilaginous tissue (Figs. 3c, 4a–d). This indicates a delay in the processes of bone formation and remodeling. At 5 weeks after fracture, the callus consisted mainly from osseous tissue without significant differences between the two groups (Figs. 3b, c, 4b, d). Although the amount of bone tissue was comparable between the two groups, in the non-stabilized fractures only woven bone was detectable, whereas fractures of the stabilized femora were bridged with lamellar bone (Fig. 4b, d).

Protein expression analysis

At 2 weeks, western blot analysis of the callus tissue demonstrated that non-stabilized femur fractures show a lower expression of BMP-2 (Fig. 5a, b). In these non-stabilized fractures the expression of collagen-2, an early

Fig. 1 Radiography of non-stabilized (a, b) and stabilized femur fractures (c, d) after 2 weeks (a, c) and 5 weeks of healing (b, d). Note the dislocated fragments and irregular callus formation of the non-stabilized fractures (a, b)



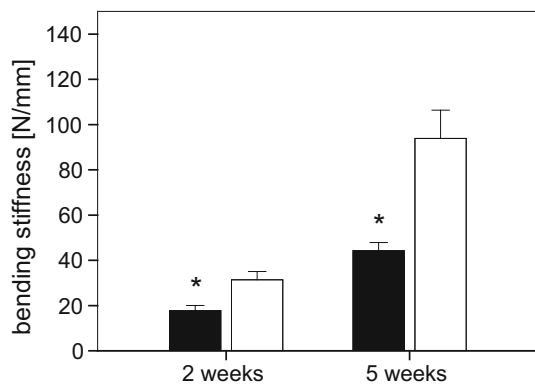


Fig. 2 Biomechanical analysis of the bending stiffness after 2 and 5 weeks of bone healing in non-stabilized (black bars) and stabilized femur fractures (white bars). Mean \pm SEM; * $p < 0.05$ vs. stabilized femur fractures

chondrocyte marker, was higher and the expression of collagen-10, a chondrocyte maturation marker which indicates mineralization of hypertrophic chondrocytes, was found slightly reduced. This difference, however, did not prove to be statistically significant (Fig. 5a, b). Analysis of CYR61 could also not detect significant differences between non-stabilization and stabilization of femur fractures (Fig. 6a, b). In contrast, the expression of VEGF was significantly lower in the callus of non-stabilized compared to stabilized fractures (Fig. 6a, b). OPG and RANKL expression were found comparable within the callus of non-stabilized and stabilized fractures (Fig. 6c, d).

Discussion

The major finding of the present study is that non-stabilization of femur fractures in mice results in delayed healing and remodeling, as indicated by a smaller amount of osseous callus tissue during the early healing period and a reduced transformation of woven bone to lamellar bone in the late period. This which was both associated with a significantly lower bending stiffness of the callus tissue when compared to that of stabilized femur fractures.

Only few studies have compared the healing process between non-stabilized and stabilized fractures in mice. Le et al. [15] analyzed the molecular mechanisms during fracture healing and could show that indian hedgehog (ihh), which regulates chondrocytes maturation, was expressed earlier and persisted longer in the callus of non-stabilized compared to stabilized fractures. At 14 days after fracture, cartilage had begun to convert to woven bone, however, with persisting hypertrophic cartilage islands expressing col-2, col-10, ihh, and ihh-induced bone morphogenetic protein-6 (BMP-6) and gli3 transcription factor (gli3) [15]. In contrast, in the 14-day callus of the stabilized fractures

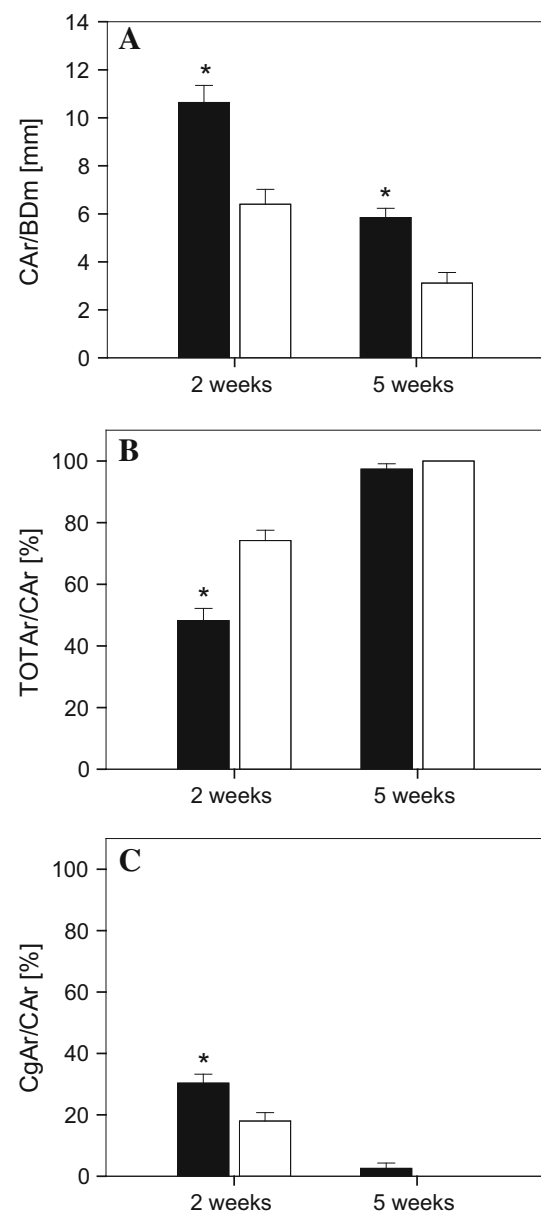


Fig. 3 Histomorphometrical analysis of the total callus area (CAr) in relation to the diameter of the femur (BDm) (a) after 2 and 5 weeks of bone healing in non-stabilized (black bars) and stabilized femur fractures (white bars). Tissue distribution within the callus as given by the total osseous tissue callus area/total callus area [TOTAr/CAr (%)] (b) and cartilaginous callus area/total callus area [CgAr/CAr (%)] (c) after 2 and 5 weeks of bone healing in non-stabilized (black bars) and stabilized femur fractures (white bars). Mean \pm SEM; * $p < 0.05$ vs. stabilized femur fractures

cartilage was largely converted to woven bone, lacking the expression of ihh, BMP-6 and gli3 [15]. These observations are in line with the histological result of the present study, demonstrating at 14 days after fracture significantly greater amounts of cartilage in the callus of non-stabilized compared to stabilized fractures.

Fig. 4 Longitudinal histological sections of femora of non-stabilized (**a, b**) and stabilized femur fractures (**c, d**) after 2 weeks (**a, c**) and 5 weeks (**b, d**) of bone healing. Scale bars represent 500 μm

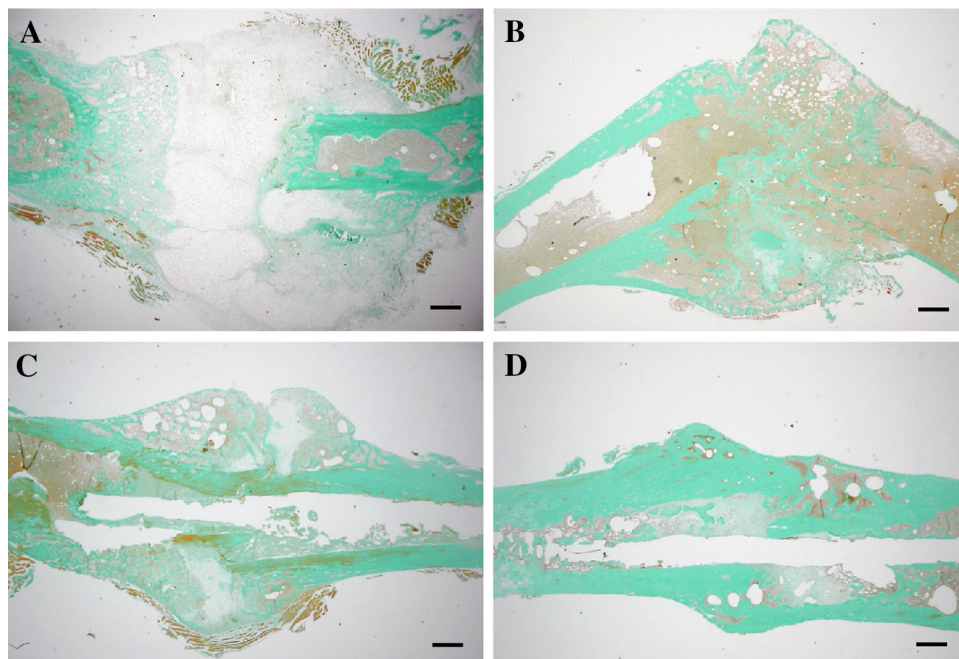
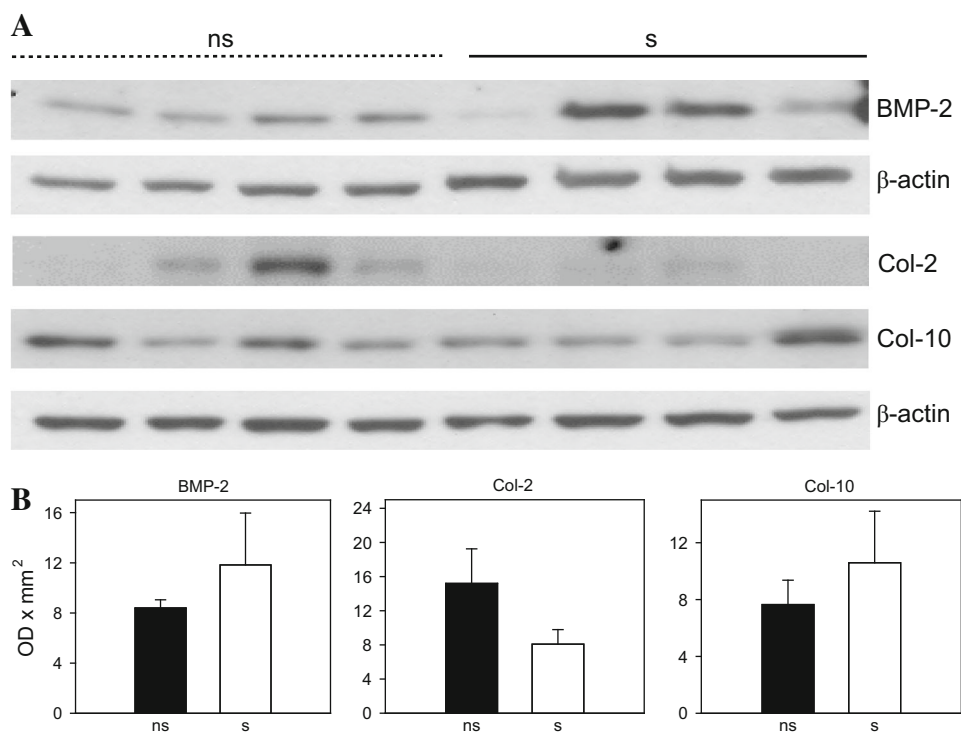


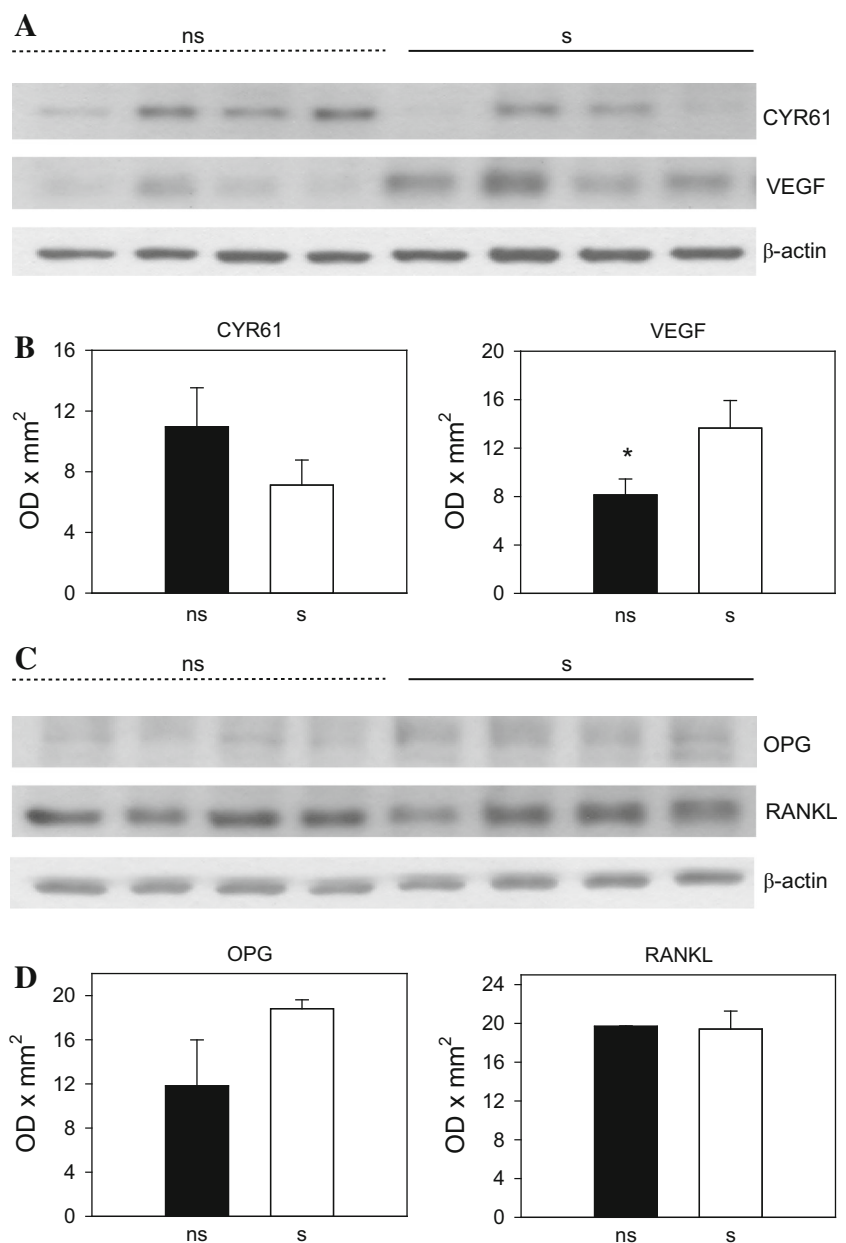
Fig. 5 Western blot analysis of the expression of BMP-2, Col-2 and Col-10 (**a, b**) in the callus of non-stabilized (ns; *black bars*) and stabilized femur fractures (s; *white bars*) after 2 weeks of bone healing. Mean \pm SEM



Although Le et al. [15] indicates that chondrocytes differentiate more rapidly in stabilized fractures, they could not observe that callus of stabilized fractures matured faster than callus of non-stabilized fractures based on their histological analyses. However, while they described that the callus of stabilized fractures at 28 days consisted of

remodeling woven bone, they do not provide information on the osseous composition of the callus of non-stabilized fractures at this stage. In addition, their study lacks a quantitative analysis of the histology and an overall analysis of callus biomechanics. Accordingly, they indicate that without a definite histological end-point at which time a

Fig. 6 Western blot analysis of the expression of CYR61 and VEGF (**a, b**) and OPG and RANKL (**c, d**) in the callus of non-stabilized (ns; *black bars*) and stabilized femur fractures (s, *white bars*) after 2 weeks of bone healing. Mean \pm SEM; * $p < 0.05$ vs. stabilized femur fractures



fracture can be considered “healed”, it remains purely speculative to conclude that stabilized fractures do not heal faster than non-stabilized ones [15].

In contrast, recent studies indicate that adequate healing of long bone fractures in mice need 4–5 weeks [5, 20]. The histomorphological analyses of the present study indicates that the callus of non-stabilized fractures not only shows a reduced amount of osseous tissue during the early healing phase, but also a lack of transformation of woven bone to lamellar bone in the late phase. Accordingly, the bending stiffness of ~ 45 N/mm at this 5 week time point was not only less than 50 % of that measured in stabilized fractures, but also

significantly lower compared to the 115–120 N/mm known from non-fractured femora in CD-1 mice [17]. Accordingly, we conclude from the present study that stabilized femur fractures in CD-1 mice heal adequately within a 5-week period, including callus ossification and remodeling, while non-stabilized femur fractures show delayed bone healing.

This view is further supported by the fact that at 14 days the significantly higher amount of cartilage within the callus tissue of non-stabilized fractures showed a higher expression of Col-2, an early cartilage marker, but a reduced expression of Col-10, which serves as a marker of chondrocyte maturation.

Because mechanical stimuli are known to be involved in angiogenesis and vascularization during fracture healing [21], some studies analyzed the effect of stability on pro-angiogenic gene expression and blood vessel formation. In vitro Ueda et al. [22] could demonstrate that shear stress applied to the surfaces of endothelial cells on collagen gel promotes and expands the growth of microvascular networks. Further on, Lu et al. [16] analyzed in vivo the early tissue vascularization and expression of angiogenesis-related genes in non-stabilized and rigidly stabilized tibia fractures in mice. They found that non-stabilized fractures had a significantly higher length density and surface density at 3 days post fracture and suggested that mechanical instability could lead to a more robust angiogenic response after fracture. However, the authors also measured VEGF at 3 and 10 days after fracture and could not detect differences between non-stabilized and stabilized fractures. This is in contrast to the results of the present study, demonstrating at day 14 a significantly reduced expression of VEGF in the callus of non-stabilized compared to stabilized fractures, suggesting a reduced vascularization. Our results are in line with that of Lienau et al. [23], demonstrating a reduced VEGF expression in tibia fractures of sheep, if supplied with a highly rotationally unstable external fixator leading to delayed healing when compared with fractures, supplied with a rigid external fixator leading to standard healing. However, apart from the expression of VEGF and the amount of microvascular network formation, it is conceivable that in non-stabilized fractures newly formed blood vessels are ruptured due to large tissue strains as a result of fragment dislocation under load. This may indeed contribute to the delayed healing of non-stabilized fractures.

In our study the CYR61 expression at day 14 was slightly higher in the callus of non-stabilized compared to stabilized fractures. This might be due to the fact that CYR61 also promotes chondrogenic differentiation. Hadjiargyrou et al. [24] could show that CYR61 expression corresponds with active chondrogenesis. They showed in a rat femur fracture model that CYR61 expression during fracture repair is regulated temporally with elevated levels at days 3 and 5 after fracture, rising dramatically at days 7 and 10 and, finally, declining at days 14 and 21. Thus, the higher CYR61 expression in the callus of non-stabilized fractures at day 14 might be related to the prolonged chondral phase, as indicated by the significantly higher amount of cartilaginous tissue.

Non-stabilization of femur fractures did not significantly affect the balance between RANKL/RANK and OPG. In the present study mechanical instability was associated with an only slightly lowered OPG expression, and did also not affect the expression of RANKL. Thus, the delayed healing of non-stabilized fractures is most probably not mediated by an inhibition of osteoclastogenesis.

In addition, non-stabilization of femur fractures may be judged critically in respect to animal welfare. During the early postoperative period, animals are markedly restricted in physical movement, which is associated with pain. In addition, each stride of the animal may result in soft tissue damage due to excessive displacements of the bone fragments. Thus, with a modern view of animal welfare we feel that non-stabilization of a femur fracture in the mouse is not an acceptable model for fracture healing studies.

In conclusion, non-stabilized femur fractures in mice show a marked delay in bone healing compared to stabilized fractures. Therefore, non-stabilized fracture models may not be used to analyze the mechanisms of normal bone healing.

Acknowledgments We thank Janine Becker for excellent technical assistance.

Compliance with ethical standards

Conflict of interest The authors have no affiliation or financial arrangement with an organization or company that has financial interests in the subject matter discussed in the manuscript.

References

- Panteli M, Pountos I, Jones E, Giannoudis PV (2015) Biological and molecular profile of fracture non-union tissue: current insights. *J Cell Mol Med* 19:685–713
- Lettin AW (1965) The effects of axial compression on the healing of experimental fractures of the rabbit tibia. *Proc R Soc Med* 58:882–886
- Nunamaker DM, Perren SM (1979) A radiological and histological analysis of fracture healing using prebending of compression plates. *Clin Orthop Relat Res* 138:167–174
- Veneroni G, Boccadoro B, Pluchino F (1962) Fixation of P-32 in the focus of a fracture and in osseous callus in the long bones in rabbits. *Arch Orthop* 75:1338–1341
- Histing T, Garcia P, Holstein JH, Klein M, Matthys R, Nuetzi R, Steck R, Laschke MW, Wehner T, Bindl R, Recknagel S, Stuermer EK, Vollmar B, Wildemann B, Lienau J, Willie B, Peters A, Ignatius A, Pohlemann T, Claes L, Menger MD (2011) Small animal bone healing models: standards, tips, and pitfalls results of a consensus meeting. *Bone* 49:591–599
- Colnot C, Thompson Z, Miclau T, Werb Z, Helms JA (2003) Altered fracture repair in the absence of MMP9. *Development* 130:4123–4133
- Tonna EA, Cronkite EP (1963) The periosteum. Autoradiographic studies on cellular proliferation and transformation utilizing tritiated thymidine. *Clin Orthop Relat Res* 30:218–233
- Garcia P, Herwerth S, Matthys R, Holstein JH, Histing T, Menger MD, Pohlemann T (2011) The LockingMouseNail—a new implant for standardized stable osteosynthesis in mice. *J Surg Res* 169:220–226
- Histing T, Holstein JH, Garcia P, Matthys R, Kristen A, Claes L, Menger MD, Pohlemann T (2009) Ex vivo analysis of rotational stiffness of different osteosynthesis techniques in mouse femur fracture. *J Orthop Res* 27:1152–1156
- Histing T, Garcia P, Matthys R, Leidinger M, Holstein JH, Kristen A, Pohlemann T, Menger MD (2010) An internal locking

- plate to study intramembranous bone healing in a mouse femur fracture model. *J Orthop Res* 28:397–402
11. Holstein JH, Matthys R, Histing T, Becker SC, Fiedler M, Garcia P, Meier C, Pohlemann T, Menger MD (2009) Development of a stable closed femoral fracture model in mice. *J Surg Res* 153:71–75
 12. Claes LE, Heigele CA, Neidlinger-Wilke C, Kaspar D, Seidl W, Margevicius KJ et al (1998) Effects of mechanical factors on the fracture healing process. *Clin Orthop* 355(Suppl):132–147
 13. Slade Shantz JA, Yu YY, Andres W, Miclau T 3rd, Marcucio R (2014) Modulation of macrophage activity during fracture repair has differential effects in young adult and elderly mice. *J Orthop Trauma* 28(Suppl 1):10–14
 14. Yu YY, Lieu S, Hu D, Miclau T, Colnot C (2012) Site specific effects of zoledronic acid during tibial and mandibular fracture repair. *PLoS ONE* 7:e31771
 15. Le AX, Miclau T, Hu D, Helms JA (2001) Molecular aspects of healing in stabilized and non-stabilized fractures. *J Orthop Res* 19:78–84
 16. Lu C, Saless N, Hu D, Wang X, Xing Z, Hou H, Williams B, Swartz HM, Colnot C, Miclau T, Marcucio RS (2011) Mechanical stability affects angiogenesis during early fracture healing. *J Orthop Trauma* 25:494–499
 17. Histing T, Stenger D, Scheuer C, Metzger W, Garcia P, Holstein JH, Klein M, Pohlemann T, Menger MD (2012) Pantoprazole, a proton pump inhibitor, delays fracture healing in mice. *Calcif Tissue Int* 90:507–514
 18. Goldberg VM, Powell A, Shaffer JW, Zika J, Bos GD, Heiple KG (1985) Bone grafting: role of histocompatibility in transplantation. *J Orthop Res* 3:389–404
 19. Gerstenfeld LC, Wronski TJ, Hollinger JO, Einhorn TA (2005) Application of histomorphometric methods to the study of bone repair. *J Bone Miner Res* 20:1715–1722
 20. Hiltunen A, Vuorio E, Aro HT (1993) A standardized experimental fracture in the mouse tibia. *J Orthop Res* 11:305–312
 21. Lienau J, Schell H, Duda GN, Seebeck P, Muchow S, Bail HJ (2005) Initial vascularization and tissue differentiation are influenced by fixation stability. *J Orthop Res* 23:639–645
 22. Ueda A, Koga M, Ikeda M, Kudo S, Tanishita K (2004) Effect of shear stress on microvessel network formation of endothelial cells with in vitro three-dimensional model. *Am J Physiol Heart Circ Physiol* 287:994–1002
 23. Lienau J, Schmidt-Bleek K, Peters A, Haschke F, Duda GN, Perka C, Bail HJ, Schütze N, Jakob F, Schell H (2009) Differential regulation of blood vessel formation between standard and delayed bone healing. *J Orthop Res* 27:1133–1140
 24. Hadjiargyrou M, Ahrens W, Rubin CT (2000) Temporal expression of the chondrogenic and angiogenic growth factor CYR61 during fracture repair. *J Bone Miner Res* 15:1014–1023